Available online at https://doi.org/10.36303/SATNT.2021cosaami.45
Conference of the South African Advanced Materials Initiative

Corrosion performance of Ti-Cu alloys targeted for biomedical applications

NDE Masia[1,2,3,a*], M Smit[1,b], IA Mwamba[1,c], L Fowler[4,d], LH Chown[2,3,e], S Norgren[4,f], C Öhman-Mägi[4,g], N Hashe[5,h], LA Cornish[2,3,i]

[1] Advanced Materials Division, Mintek, Randburg 2125, South Africa
[2] School of Chemical and Metallurgical Engineering, University of the Witwatersrand, Johannesburg 2050, South Africa
[3] DST-NRF Centre of Excellence in Strong Materials, hosted by the University of the Witwatersrand, Johannesburg 2050, South Africa
[4]Division of Applied Materials Science, Department of Engineering Sciences, The Ångström Laboratory, Uppsala University, Box 534, 751 21 Uppsala, Sweden
[5]Department of Physics, Nelson Mandela University (NMU), Port Elizabeth, South Africa
Email: [a]nomsombulukoh@mintek.co.za, [b]melanies@mintek.co.za, [c]alainm@mintek.co.za, [d]fowler.lee8@gmail.com, [e]dlesleyhchown@gmail.com, [f]susanne.m.norgren@sandvik.com, [g]caroline.ohman@angstrom.uu.se, [h]Nobom.Hashe@mandela.ac.za, [i]lesley.cornish@wits.ac.za*

Abstract

The Thermo-Calc™ program and TTTI3 database were used to predict the phases in Ti-Cu with 5, 25, and 40 wt% Cu. Based on the predicted results, experimental work was conducted and the Ti-Cu alloys were produced in a button arc furnace, and characterised in the as-cast and the annealed condition (900°C) followed by water quenching. Microstructures and compositions were determined using an electron probe micro-analyser, and the phases were identified by X-ray diffraction. The corrosion performance was measured by potentiodynamic polarisation in a phosphate buffered saline solution at 37°C at 7.4 pH while purging with nitrogen gas. The Ti-5Cu and Ti-25Cu alloys comprised (αTi) and Ti_2Cu phases, the Ti-40Cu alloy comprised Ti_2Cu and TiCu. Although the addition of copper decreased the corrosion performance by down to 75%, the corrosion rates were still within the acceptable range (0.02-0.13 mm/y) for biocompatibility of metallic implants. Annealing at 900°C did not improve the corrosion performance.

1. Introduction

Commercially pure titanium (CP Ti) and titanium alloys are widely used in dental implant applications due to their good mechanical strength, successful osseointegration, high strength-to-weight ratio and resistance to corrosion.[1,2,3] Corrosion of titanium dental implants is associated with implant failure and is considered as a trigger factor for peri-implantitis,[4] which is an inflammatory disease affecting the surrounding tissues of the implant, predominately the bone.[4,5] It is caused by the adhesion of pathogenic biofilms on the implant surface and peri-implant tissues, resulting in bone loss and destruction of soft tissues.[4] Surgical and non-surgical treatments performed to control peri-implantitis have been ineffective, and avoiding bacteria adhesion with hydrophilic coatings inhibits tissue integration.[6,7] An alternative approach to antibacterial treatment are gels containing carvacrol and thymol,[8] while others studied the antimicrobial affinity of different inorganic ions.[7] Silver and copper have emerged as promising alloying elements for antibacterial materials.[7] However, silver may lead to DNA damage and cannot kill bacteria at lower pH levels and temperatures.[7,9] Due to these limitations, addition of copper is being studied. Addition of copper to titanium alloys which increases antibacterial properties has more potential.[10] The antibacterial property was associated with preferential copper ion release from the Ti-Cu alloys due to the galvanic corrosion between phases with copper and the titanium matrix. This galvanic coupling is strong and stable for copper contents above 5 wt%. They also obtained higher corrosion resistance of Ti-Cu alloys compared to CP Ti.[11] It was thought that the phases with copper such as Ti_2Cu played a very important role in the strong antibacterial behavior.[12] Heat treatment, such as annealing and ageing, could also significantly improve the mechanical properties, corrosion resistance and antibacterial rate due to the redistribution of copper and size distribution of Ti_2Cu precipitates.[13] Although Ti-Cu alloys have high corrosion resistance due to TiO_2 formed on the surfaces, they are not immune to corrosion. The aim of this study was to assess the effect of the Ti_2Cu compound and its proportions on the corrosion resistance, to see whether there was a degradation or improvement, and to relate the effect to the amounts of Ti_2Cu. Grade 4 CP Ti was selected due to its higher tensile strength and yield strength than Grades 1 to 3.

2. Materials and experimental procedure

2.1 Material selection and preparation

CP Titanium Grade 4 (15mm diameter rod, Multi Alloys (Pty) Ltd) and high purity copper (SAE CA110 - 3 mm thick plate, Meglan Trading CC) were the starting materials, and Table 1 shows their compositions. Ti-Cu alloys of 5, 25, and 40 wt% Cu were produced in a button arc melting furnace, with a high-energy arc at high temperatures on a water-cooled copper hearth. Two melts of each alloy were prepared: one melt was left as-cast and the other was annealed. The annealing was done in sealed quartz ampoules (each sample being in a separate ampoule) at 1.333 mbar in an induction furnace at 900°C for 2 h, followed a fast water quench (by crushing the amploules on quenching) to retain the (βTi) phase. Figure 1 shows the alloys on the Ti-Cu phase diagram.[9]

Table 1: Chemical compositions of titanium and copper as starting materials

	Elements (wt%)							
	N	**C**	**O**	**Fe**	**Ag**	**H**	**Cu**	**Ti**
Titanium Gr 4	0.05	0.08	0.4	0.5	-	0.015	-	98.96
SAE CA110	-	-	0.04	-	0.05	-	99.91	-

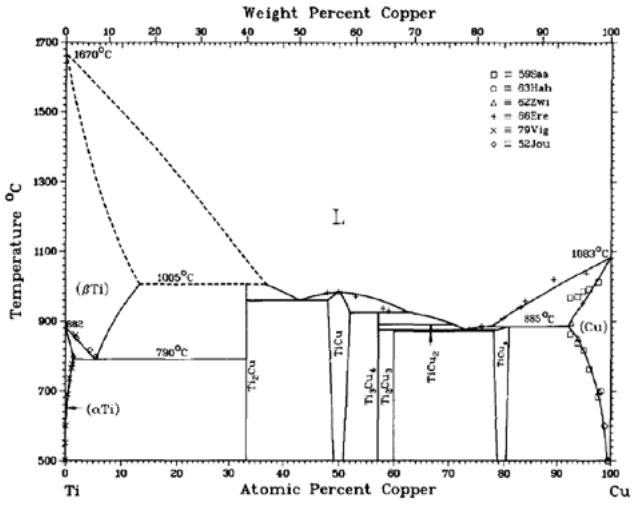

Figure 1: Ti-Cu phase diagram[14]

2.2 Material characterisation

Characterisation was performed on all the alloys in the as-cast and annealed conditions to study the basic features before corrosion testing. Chemical composition and microstructures were analysed using a JEOL 8230 electron probe microanalyser, with a combination of up to 5 wavelength dispersive X-ray spectroscopy (WDS) detectors and an energy dispersive X-ray spectroscopy (EDS) detector. Analyses were performed at 20 kV, 30 nA, and calibrated using pure metal reference standards. X-ray diffraction (XRD) was performed using a Bruker D8 Advance powder diffractometer, with a Linxeye detector using Fe filtered Co-Kα radiation. This method uses the net intensity of the main peaks of the phases, and identification is based on the crystal structure of phases that occur in amounts of >3 mass %. Amorphous phases are not detected, so the phases specified may not necessarily have the compositions deduced.

3. Electrochemical testing

The corrosion tests were performed at 37±1°C (human body temperature) in a phosphate buffered saline (PBS) solution at pH 7.4. The PBS solution was chosen due to its buffer properties and because it has similar ion concentration to some human body fluids (isotonic).[15] Table 2 shows the composition of the PBS solution. Electrochemical tests were open circuit potential (OCP) and potentiodynamic polarization tests. Potentiodynamic tests were undertaken according to the ASTM-G5-2013 Standard, using a PC driven "ACM Gill AC" potentiostat. The alloys were sectioned into 10x10mm samples and were inserted in a sealed PVC holder. One graphite rod acted as a counter-electrode and a Haber-Luggin capillary made the junction with a saturated calomel reference electrode (SCE). All potential values were measured with respect to the SCE. Nitrogen was bubbled continuously through the solution during testing to create an anaerobic environment, simulating conditions in the mouth.

The OCP was determined when the electrodes were immersed in the solution and the potential was recorded as a function of time. It was recorded at two hours when the potential was stable (at equilibrium). When the OCP was stable, potentiodynamic polarisation tests were done for each alloy. Each scan was from –250 mV to +1500 mV versus the corrosion potential at a scanning speed of 10 mV/min. The corrosion current densities were determined by Tafel extrapolation of the rate-determining segment of the polarisation curve, and the corrosion rates were calculated using Equation 1:

$$\text{Corrosion rate (mm/y)} = 0.009 \times I_{Corr} \times EW/d \qquad \text{Equation 1}$$

where mm/y = millimetres per year, EW = equivalent weight of the corroding species in grams (g), d = density of the corroding species (g/cm³), and I_{Corr} = corrosion current density (µA/cm²).

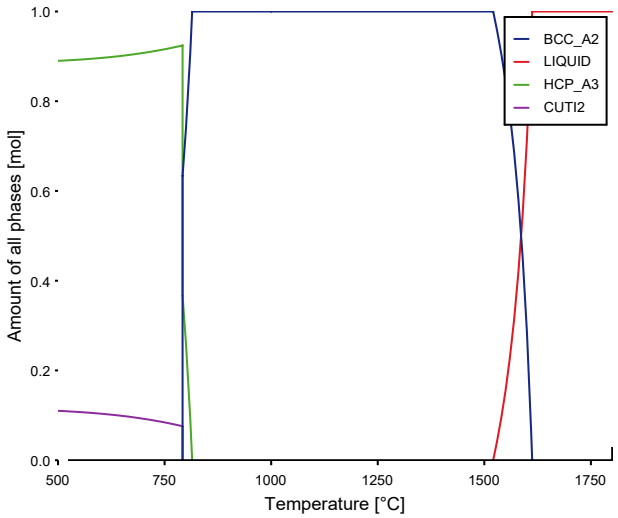

Figure 2: Phase proportion diagram for Ti-5Cu

Table 2: Chemical composition of the PBS solution

Reagents (g)			
Sodium chloride (NaCl)	Potassium chloride (KCl)	Sodium hydrogen phosphate (Na_2HPO_4)	Potassium dihydrogen phosphate (KH_2PO_4)
8	0.2	1.44	0.24

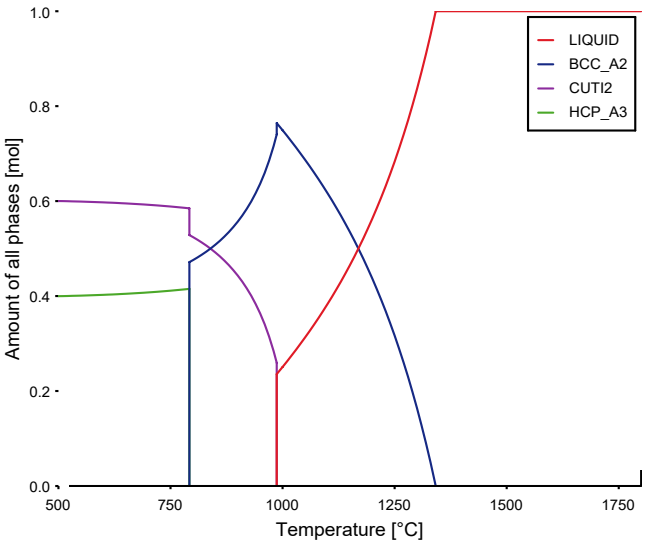

Figure 3: Phase proportion diagram for Ti-25Cu

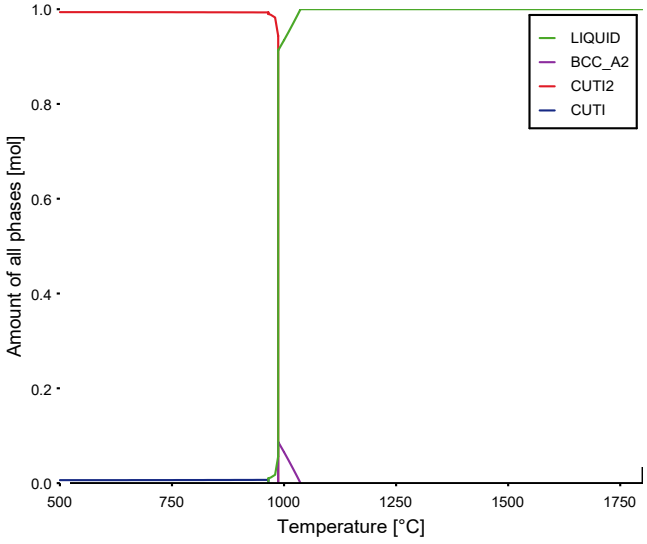

Figure 4: Phase proportion diagram for Ti-40Cu

of phases as a function of temperature for all the alloys. Ti-5Cu

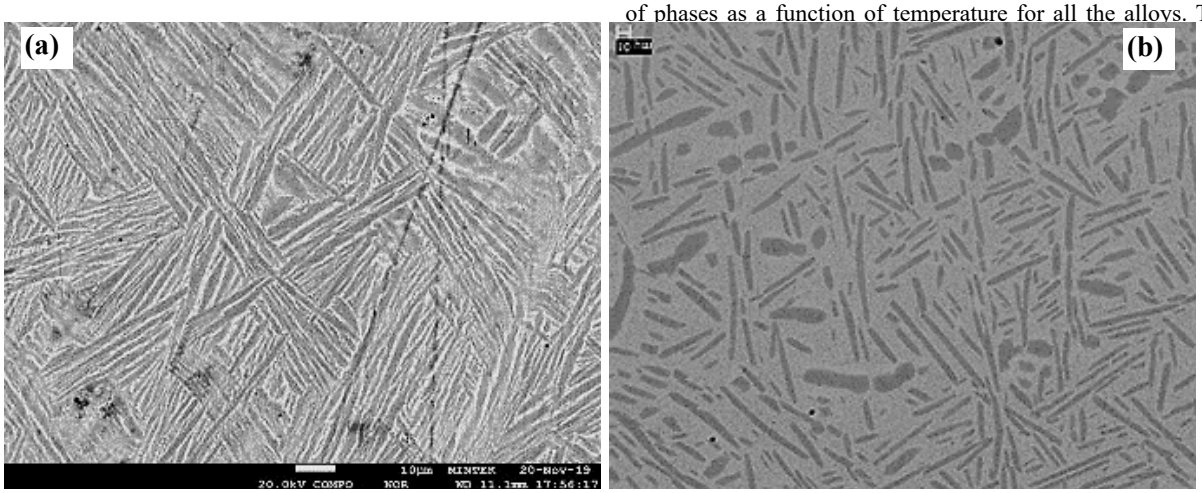

Figure 5: SEM-BSE images of Ti-5Cu: (a) as-cast, and (b) annealed at 900°C, showing (αTi) (dark contrast) and (βTi) (light contrast)

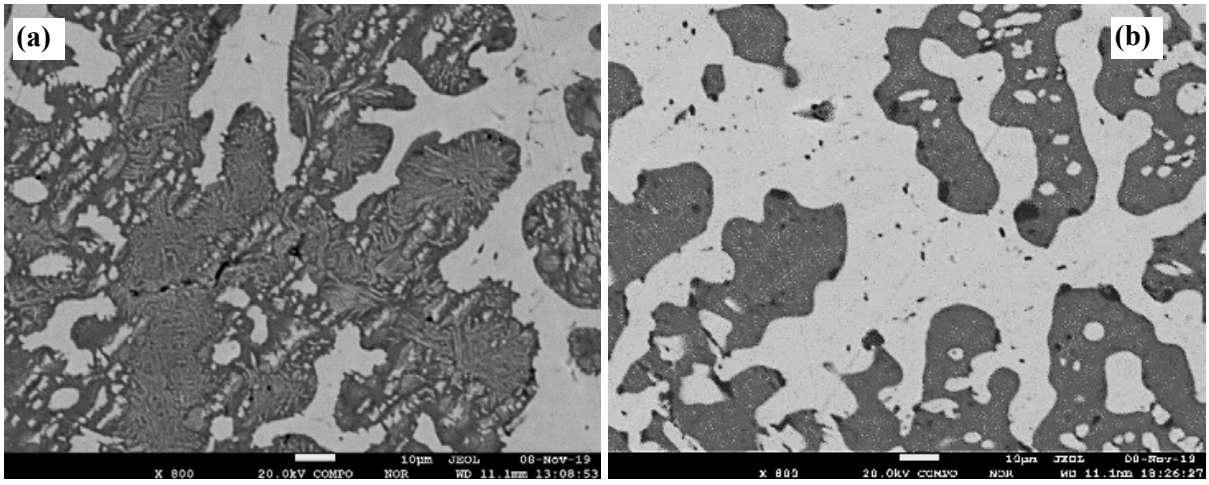

Figure 6: SEM-BSE images of Ti-25Cu: (a) as-cast, and (b) annealed at 900°C, showing (αTi) (dark contrast) and Ti_2Cu (light contrast)

4. Results and discussion

4.1 Thermo-Calc results

Thermo-Calc predicted the equilibrium phases: liquid, BCC (βTi), HCP (αTi), Ti_2Cu and TiCu. Figures 2 to 4 show the mole fractions and Ti-25Cu alloys were predicted to comprise BCC (βTi), HCP (αTi) and Ti_2Cu phase, while the Ti-40Cu alloy was predicted to comprise BCC (βTi), Ti_2Cu and TiCu.

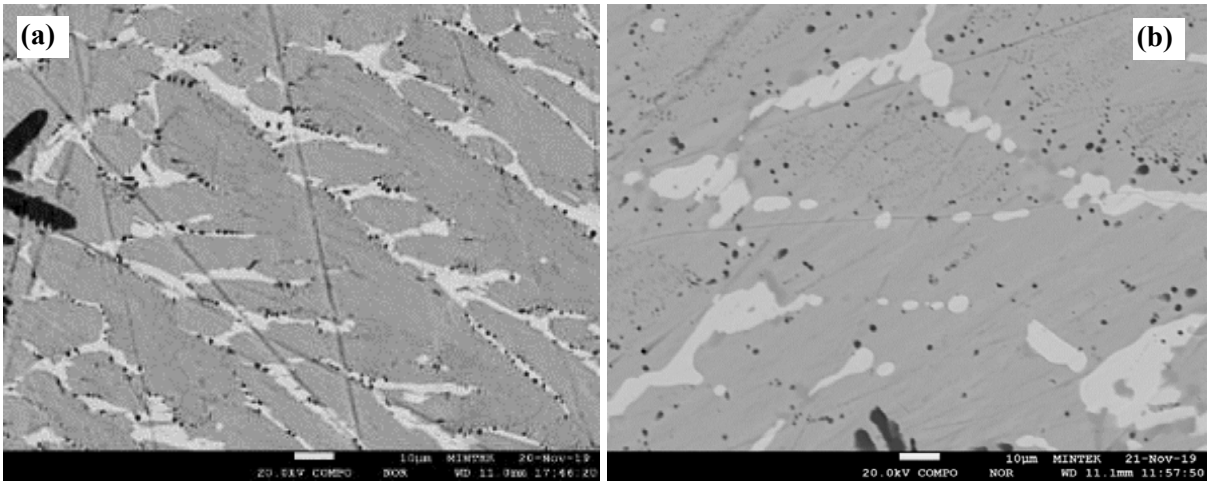

Figure 7: SEM-BSE images of Ti-40Cu: (a) as-cast, and (b) annealed at 900°C, showing Ti oxides (very dark contrast), Ti_2Cu (medium contrast) and TiCu (light contrast)

Table 3: EDX analyses

Alloy	Cu (wt%)			
	Phase		As-cast	900°C
Ti-5Cu	Overall		4.6±*0.9*	4.7±1.0
	Dark	(αTi)	2.3±0.5	2.7±0.9
	Light	(βTi)	6.2±0.9	6.8±2.1
Ti-25Cu	Overall		26.2±2.0	24.9±3.8
	Dark	(*β*Ti)	11.3±0.1	12.0±1.7
	Light	Ti_2Cu	37.0±0.5	38.0±0.1
	Precipitates in dendrites		None	18.1±1.5
Ti-40Cu	Overall		39.1±5.2	39.5±8.2
	Dark	Ti_2Cu	39.5±0.2	38.6±0.9
	Light	TiCu	55.6±0.2	56.2±0.1

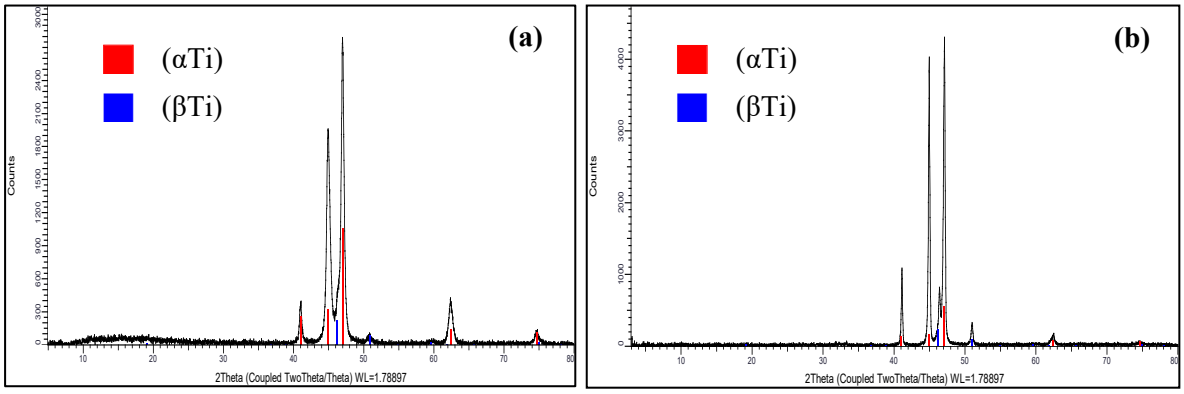

Figure 8: XRD patterns of Ti-5Cu: (a) as-cast, and (b) annealed at 900°C

4.2 Microstructures and analyses

SEM-BSE images show differences in average atomic number: higher average atomic number phases have lighter contrasts.[16] Copper appears lighter since it has a higher atomic number than titanium. As-cast Ti-5Cu comprised lamellar (αTi) + (βTi), whereas the annealed alloy had (αTi) precipitated in (βTi), Figure 5. The EDX analysis indicated that the dark phase was (αTi), and light phase was (βTi), Table 3, which was retained,[17] and agreed with XRD for both as-cast and annealed alloys, Figure 8.

Ti-25Cu alloys comprised dark dendrites in a Ti_2Cu matrix, Figure 6 and Table 3. After annealing at 900°C, light precipitates occurred inside the dendrites. The EDX analysis indicated the dark dendrites to be (βTi) instead of (αTi) and the matrix to be Ti_2Cu. The XRD patterns confirmed (αTi) and Ti_2Cu phases for both as-cast and annealed alloys, Figure 9.

Ti-40Cu comprised small oxide dendrites inside the Ti_2Cu dendrites, which were surrounded by the TiCu matrix, Figure 7. The dark phase had less copper than the light phase, Table 3. The XRD patterns confirmed Ti_2Cu and TiCu phases for both as-cast

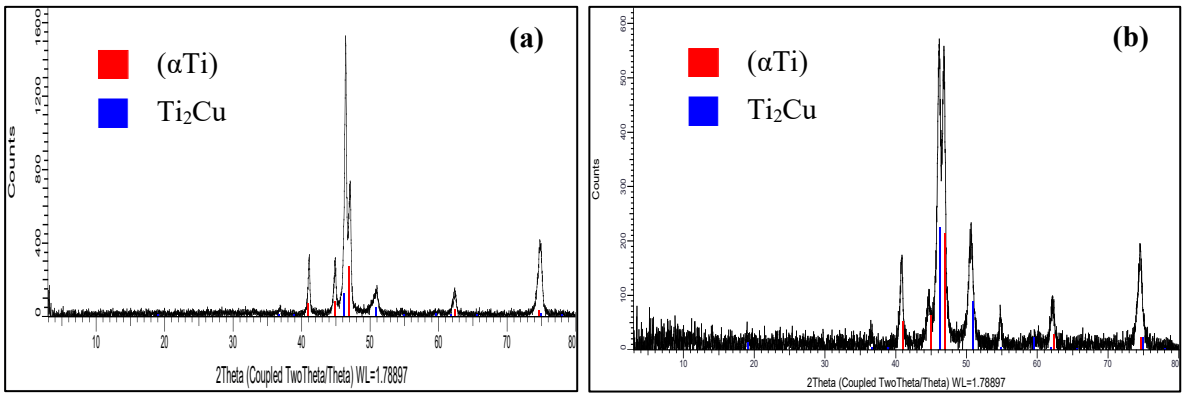

Figure 9: XRD patterns of Ti-25Cu: (a) as-cast, and (b) annealed at 900°C

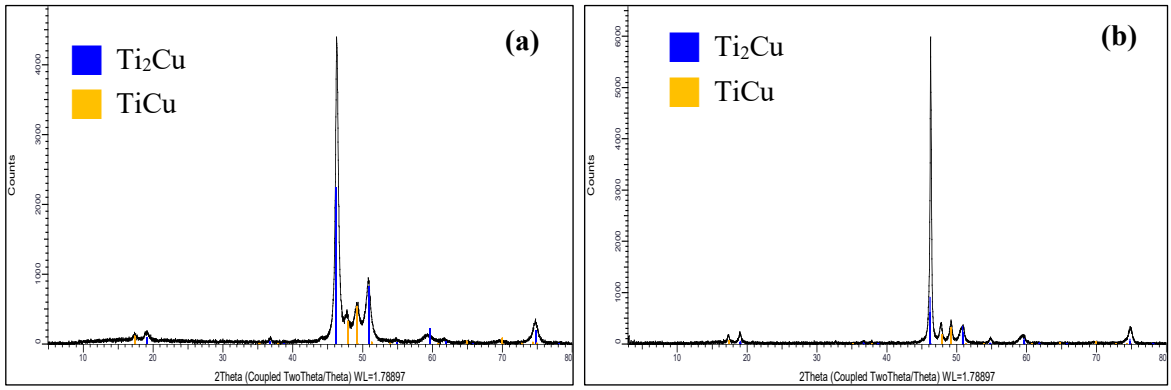

Figure 10: XRD patterns of Ti-40Cu: (a) as-cast, and (b) annealed at 900°C

and annealed alloys, Figure 10. As well as there being more Ti_2Cu in the microstructure, the relative peak intensity of Ti_2Cu increased with more copper, indicating that more Ti_2Cu phase formed, Figure 8 to Figure 10.

5. Electrochemical testing

Figure 11 and Table 4 show the OCP results. At two hours the OCP of the samples stabilised, although alloys Ti-25Cu and Ti-40Cu in the as-cast condition showed an initial increase in OCP, indicating that the passive layer was formed quickly on the surfaces. Higher copper additions shifted OCP in more noble positions (The OCP shift in the noble direction for the alloys suggests the formation of a passive film that reduces the corrosion rate) than for Ti-5Cu, while annealing at 900°C shifted the OCP towards less noble positions.

Figure 12 shows the potentiodynamic polarisation scans. Figure 13 shows the corrosion rates obtained and Table 4 gives the overall results. Ti-25Cu and Ti-40Cu alloys in both the as-cast and annealed conditions showed an increase in corrosion rate, with Ti-25Cu alloy showing a higher corrosion rate than the other alloys. This indicates that increasing copper content in the alloys decreased the corrosion resistance. Previously,[18] the corrosion rate of as-cast CP Ti was 0.00059 mm/y, thus as-cast Ti-25Cu had the highest corrosion rate. The effect of alloy copper content associated

Table 4: Potentiodynamic polarisation corrosion rates of as-cast and annealed Ti-5Cu, Ti-25Cu and Ti-40Cu alloys in PBS solution

Samples		OCP (mV SCE)	E_{corr} (mV SCE)	i_{corr} (mA/cm²)	Corrosion rates (mm/y)	
					Individual	Average
Ti-5Cu	As-cast	-711	-740	3.0 x 10^{-5}	0.00027	0.00027±0.0
		-659	-740	3.0 x 10^{-5}	0.00027	
	Annealed at 900°C	-729	-754	2.8 x 10^{-5}	0.00025	0.00026±0.0
		-374	-398	3.1 x 10^{-5}	0.00028	
Ti-25Cu	As-cast	-592	-728	7.4 x 10^{-5}	0.00067	0.00063±0.0
		-571	-718	6.8 x 10^{-5}	0.00061	
	Annealed at 900°C	-784	-928	1.0 x 10^{-4}	0.00090	0.00090±0.0
		-792	-928	1.0 x 10^{-4}	0.00090	
Ti-40Cu	As-cast	-357	-363	4.0 x 10^{-5}	0.00036	0.00036±0.0
		-448	-442	3.9 x 10^{-5}	0.00035	
	Annealed at 900°C	-748	-889	9.1 x 10^{-5}	0.00082	0.00086±0.0
		-662	-803	1.0 x 10^{-4}	0.00090	

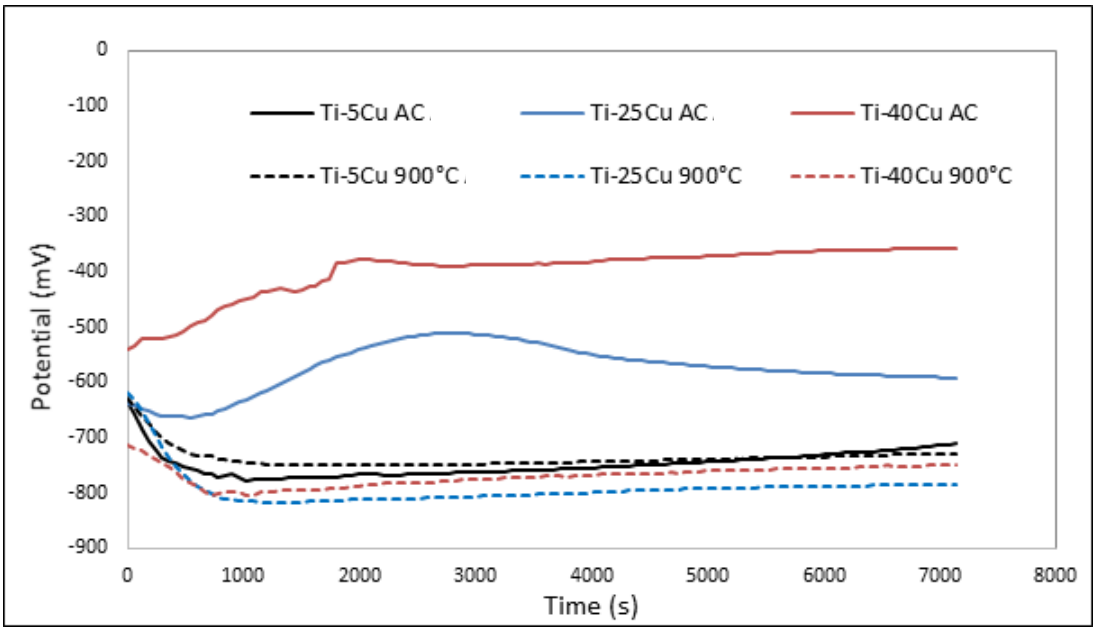

Figure 11: OCP plots for as-cast and annealed Ti-5Cu, Ti-25Cu and Ti-40Cu alloys in PBS solution

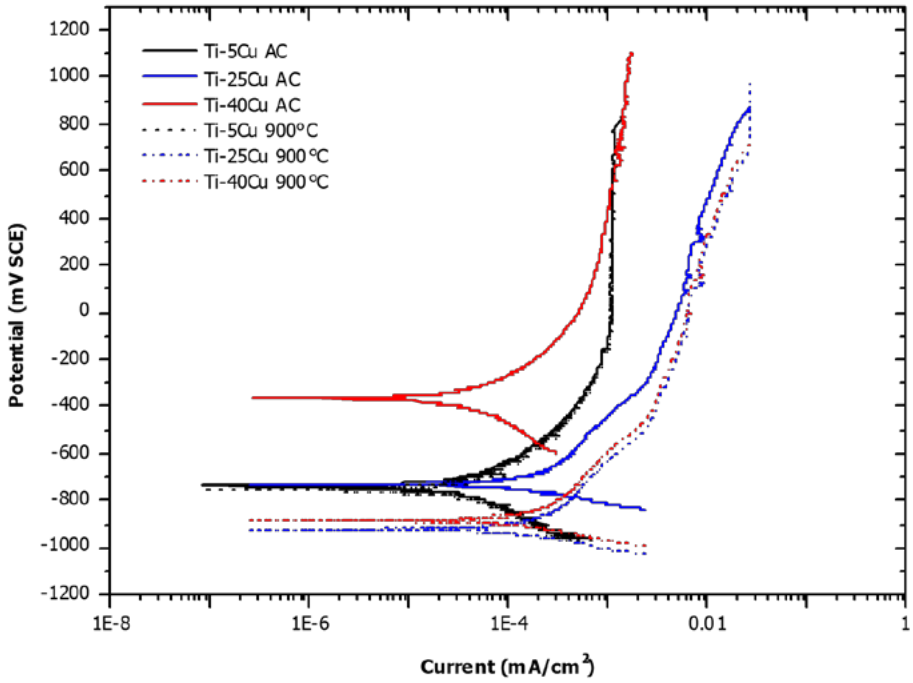

Figure 12: Potentiodynamic polarisation scans of as-cast and annealed Ti-5Cu, Ti-25Cu and Ti-40Cu alloys in PBS solution

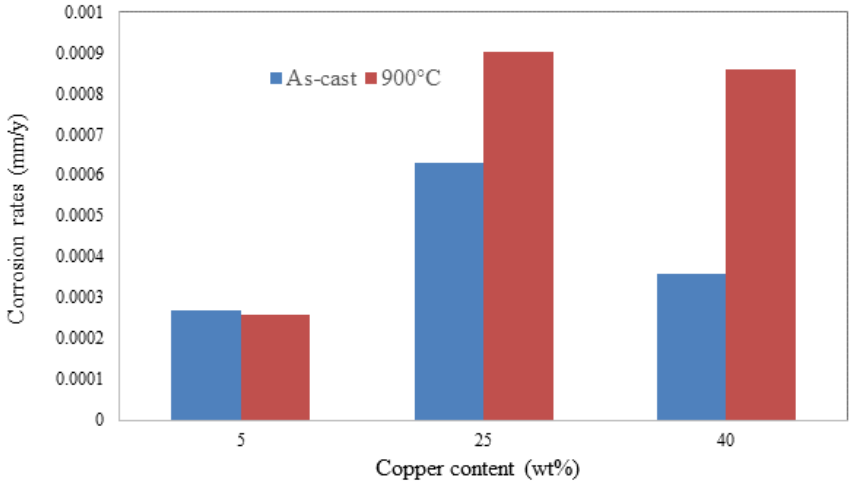

Figure 13: Corrosion rates of as-cast and annealed Ti-5Cu, Ti-25Cu and Ti-40Cu alloys in PBS solution

with the intermetallic compounds has also been observed for Ti–Cu alloys by Osório et al.,[19] who concluded, for their alloys, that with increased alloy copper content, the volumetric fraction of Ti_2Cu also increased, i.e., with lower copper content, a more homogeneous and smoother oxide film formed.[19] The impedance parameters made it clear that an intact passive titanium oxide film had been formed.

The annealed Ti-25Cu and Ti-40Cu alloys had higher corrosion rates, but alloy Ti-5Cu had a slightly reduced corrosion rate. Pina et al.[15] also reported increased current density with increased copper content in Ti-Cu alloys. The corrosion rate of CP Ti annealed at 900°C was 0.00108 mm/y[18] which was lower than Ti-25Cu and Ti-40Cu, although their corrosion rates were still acceptable for biomaterial applications.[20] All samples showed an active to passive behaviour, with no pitting breakdown. A long passivation stage in the Tafel curves of all the alloys indicated good passivation protection on the surface, which showed that neither copper additions nor annealing reduced the passivation protection. No pitting or localised attack was observed after testing. Ti-5Cu alloy at both conditions had higher corrosion resistance than the other alloys. The potentiodynamic polarisation tests showed that corrosion rates obtained were very low, below 0.13mm/y which is an acceptable corrosion rate for biomaterial design and application.[20] However, since Cu ions in liquid solution promote the antimicrobial activity, some corrosion is necessary to allow the Cu ions to be available.[21]

6. Conclusions

This study assessed the corrosion performance of Ti-Cu Alloys targeted for biomedical applications, and the following conclusion were made:

- XRD gave similar results to Thermo-Calc: where Ti-5Cu and Ti-25Cu comprised (αTi) and Ti_2Cu, while Ti-40Cu comprised Ti_2Cu and TiCu.
- The as-cast Ti-5Cu alloy had a lamellar (αTi) and (βTi) microstructure, and after annealing (αTi) was precipitated in (βTi). Ti-25Cu alloys comprised dark (αTi) dendrites in a Ti_2Cu matrix and after annealing, light precipitates occurred inside the dendrites. Ti-40Cu comprised small oxide dendrites inside the Ti_2Cu dendrites, which were surrounded by the TiCu matrix, for both as-cast and annealed alloys.
- All samples showed active-to-passive behaviour without pitting breakdown. Long passivation stages existed for all alloys, indicating that copper did not destroy the passivation protection. The best alloy was Ti-5Cu. The corrosion rates were very low, below 0.13 mm/y, which although higher than Grade 4, is still an acceptable corrosion rate for biomaterial design and application. It is unlikely that improvements need to be made to this because some Cu in solution is needed for the antimicrobial properties. The corrosion performance of CP Ti alloyed with copper was acceptable for biomedical implants. The next stage of this work should include mechanical properties, anti-bacterial testing, then osseointergration studies.

Acknowledgments

The authors would like to acknowledge Mintek, University of the Witwatersrand, Uppsala University, NRF and Nelson Mandela University for assistance during the project and approval to publish this work.

References

1. C. Schmidt, I. Anita and L. Claes, "Proliferation and differentiation parameters of human osteoblasts on titanium and steel surfaces," *Journal of Biomed Mater Res,* vol. 54, p. 209–215, 2001.
2. S. G. S. Gosavi and R. Alla, "Titanium: A Miracle Metal in Dentistry," *Trends Biomaterial Artificial Organs,* vol. 27, no. 1, pp. 42-46, 2013.
3. H. e. a. Ananth, "A Review on Biomaterials in Dental Implantology," *International Journal of Biomedical Science ,* vol. 11, no. 3, pp. 113-120, 2015.
4. D. Rodrigues, P. Valderrama, T. Wilson, K. Palmer, A. Thomas, S. Sridhar, A. Adapalli, M. Burbano and C. Wadhwani, "Titanium Corrosion Mechanisms in the Oral Environment: A Retrieval Study," *Materials,* vol. 6, pp. 5258-5274, 2013.
5. M. Soler, S. Hsu, C. Fares, F. Ren, R. Jenkins, L. Gonzaga, A. Clark, E. O'Neill, D. Neal and J. Esquivel-Upshaw, "Titanium Corrosion in Peri-Implantitis," *Materials,* vol. 13, no. 23, p. 5488, 2020.
6. J. Prathapachandran and N. Suresh, "Management of peri-implantitis," *Dental Research Journal,* vol. 9, no. 5, p. 516–521, 2012 .
7. L. Fowler, O. Janson, H. Engqvist, S. Norgren and C. Öhman-Mägi, "Antibacterial investigation of titanium-copper alloys using luminescent Staphylococcus epidermidis in a direct contact test," *Mater Sci Eng C Mater Biol Appl,* vol. 97, pp. 707-714, 2019.
8. M. Memara, P. Raei, N. Alizadeh, M. Aghdam and H. Kafil, "Carvacrol and thymol: strong antimicrobial agents against resistant isolates," *Medical Microbiology,* vol. 28, p. 63–68, 2017.
9. K. Bruellhoff, J. Fiedler, M. Möller, J. Groll and R. Brenner, "Surface coating strategies to prevent biofilm formation on implant surfaces," *The International Journal of Artificial Organs,* vol. 33, no. 9, pp. 646-53, 2010.
10. E. Zhang, X. Wang, M. Chen and B. Hou, "Effect of the existing form of Cu element on the mechanical properties,bio-corrosion and antibacterial properties of Ti-Cu alloys for biomedical application," *Materials Science and Engineering C,* vol. C, no. 69, pp. 1210-1221, 2016.
11. J. Liu, F. Li, C. Liu, H. Wang, B. Ren and K. Yang, " Effect of Cu content on theantibacterial activity of titanium-copper sintered alloys," *Mater. Sci. Eng. CMater. Biol.,* no. App.35, p. 392–400, 2014.
12. E. Zhang, X. Wang, M. Chen and B. Hou, "Effect of the existing form of Cu element on the mechanical properties, bio-corrosion and antibacterial properties of Ti-Cu alloys for biomedical application," *Materials Science and Engineering C,* no. 69, p. 1210–1221, 2016.
13. M. Bao, Y. Liu, X. Wang, L. Yang, S. Li, J. Ren, G. Qin and E. Erlin Zhanga, "Optimization of mechanical properties, biocorrosion properties and antibacterial properties of wrought Ti-3Cu alloy by heat treatment," *Bioactive Materials,* vol. 3, no. 1, pp. 28-38, 2018.
14. J. Murray, "The Cu-Ti (Copper-Titanium) system," *Bullet of Alloy Phase Diagrams,* vol. 4, no. 1, pp. 81-95, 1983.
15. S. Cabeza, P. Zubiaur, G. Garcés, C. Andrade and P. Adeva, "Corrosion Behaviour of Mg98.5Nd1Zn0.5 (at. %) Alloy in Phosphate Buffered Saline Solution," *Metals,* vol. 10, no. 148, pp. 1-16, 2020.
16. A. Nanakoudis, "https://www.thermofisher.com/blog/microscopy/sem-signal-types-electrons-and-the-information-they-provide/," ThermoFisher, 21 November 2019. [Online]. [Accessed 16 September 2021].
17. D. Brice, "AN ASSESSMENT OF UNCOMMON TITANIUM BINARY SYSTEMS:Master of Science (Material Science and Engineering)," UNIVERSITY OF NORTH TEXAS, USA, 2015.
18. N. Masia, L. Chown, M. Smit, A. Mwamba and L. Cornish, "Influence of copper on the corrosion properties of Grade 4 titanium for biomedical applications [Poster}," University of witwatersrand, Johannesburg, 2019.
19. W. Osórioa, F. C. R. Caramb and A. Garcia, "The role of Cu-based intermetallics on the pitting corrosion behavior of Sn–Cu, Ti–Cu and Al–Cu alloys," *Electrochimica Acta,* vol. 77, p. 189–197, 2012.
20. R. Bhola, S. Bhola, B. Mishra and D. Olson, "Corrosion in Titanium Dental Implants/Prostheses - A Review," *Trends Biomater. Artif. Organs,* pp. 34-46, 2011.
21. j. Jiao, S. Zhang, X. Qu and B. Yue, "Recent Advances in Research on Antibacterial Metals and Alloys as Implant Materials," *Frontiers in Cellular and Infection Microbiology,* vol. 11, no. Article 693939, pp. 1-19, 2021.